ELSEVIER

Journal of Photochemistry and Photobiology A: Chemistry 109 (1997) 177–183

Journal of PHOTOCHEMISTRY AND PHOTOBIOLOGY A: CHEMISTRY

# Phenol decomposition using $M^{n+}/TiO_2$ photocatalysts supported by the sol–gel technique on glass fibres

V. Brezová *, A. Blažková, Ľ. Karpinský, J. Grošková, B. Havlínová, V. Jorík, M. Čeppan

*Slovak Technical University, Faculty of Chemical Technology, Radlinského 9, SK-812 37 Bratislava, Slovak Republic*

Received 19 November 1996; accepted 25 March 1997

**Abstract**

The photoactivity of supported $TiO_2$ and $M^{n+}/TiO_2$ ($M^{n+} \equiv Li^+$, $Zn^{2+}$, $Cd^{2+}$, $Ce^{3+}$, $Co^{3+}$, $Cr^{3+}$, $Fe^{3+}$, $Al^{3+}$, $Mn^{2+}$ and $Pt^0$) layers, fixed on glass fibres by the sol–gel technique, was tested using the reaction of phenol degradation. The concentration of metal dopant in the immobilized photocatalysts was 5 mol.% $M^{n+}:Ti^{4+}$. In addition, the effect of platinum loading in $Pt^0/TiO_2$ samples ($Pt^0$ content in the range 0.5–5.0 mol.% $Pt^0:Ti^{4+}$) was investigated. The prepared materials were also characterized by their isoelectric points and reflectance spectra. The photoactivity of the materials prepared is strongly dependent on the character and concentration of the dopant. The best results in terms of phenol decomposition were obtained for dopant-free $TiO_2$, $Li^+/TiO_2$, $Zn^{2+}/TiO_2$ and $Pt^0/TiO_2$ (Pt content, less than 5 mol.% $Pt^0:Ti^{4+}$). However, using $Pt^0/TiO_2$ layers, we observed a slower decomposition of hydroquinone, which is produced as an intermediate by phenol hydroxylation. The presence of $Co^{3+}$, $Cr^{3+}$, $Ce^{3+}$, $Mn^{2+}$, $Al^{3+}$ and $Fe^{3+}$ ions in the $TiO_2$ photocatalyst (5 mol.% $M^{n+}:Ti^{4+}$) has a detrimental effect on its photoactivity. © 1997 Elsevier Science S.A.

*Keywords:* Glass fibres; $M^{n+}/TiO_2$ photocatalysts; Phenol decomposition; Sol–gel technique

## 1. Introduction

The photocatalytic mineralization of organic pollutants using active $TiO_2$ photocatalysts has been established as an effective method for water and air purification [1–4]. However, the use of powdered photocatalysts in technological applications may produce difficulties during processing. Consequently, recent investigations have focused on the preparation of immobilized, active $TiO_2$ layers on suitable supporting materials [5–12]. $TiO_2$ layers have been successfully prepared by the sol–gel process [7–11]. Their structure and photochemical activity are strongly dependent on the temperature processing during preparation [8,11,13].

The incorporation of metal ions in $TiO_2$ photocatalysts may substantially alter their photocatalytic activity [14–20]. In addition, the bulk and surface properties and the photoactivity are strongly dependent on the methods used for photocatalyst formation. The dominant parameters include the character and concentration of the dopant and the thermal treatment [15,17].

In this study, we prepared $TiO_2$ and $M^{n+}/TiO_2$ ($M^{n+} \equiv Li^+$, $Zn^{2+}$, $Cd^{2+}$, $Ce^{3+}$, $Cr^{3+}$, $Co^{3+}$, $Fe^{3+}$, $Al^{3+}$, $Mn^{2+}$ and $Pt^0$) layers fixed on glass fibres by the sol–gel technique. The concentration of metal dopant in the fixed photocatalysts was 5 mol.% ($M^{n+}:Ti^{4+}$). In addition, for $Pt^0/TiO_2$, we synthesized materials with metal concentrations of 0.5, 1.25, 2.5 and 3.75 mol.% ($Pt^0:Ti^{4+}$). The photocatalytic activity of the supported photocatalysts was tested using the reaction of phenol degradation.

## 2. Experimental details

### 2.1. Chemicals

Titanium(IV) tetrabutoxide ($Ti[O(CH_2)_3CH_3]_4$; 99%) and ethyl acetoacetate (99%) were purchased from Aldrich. Methanol (quality for gas chromatography), ethanol (spectroscopic grade), nitric acid and phosphoric acid were obtained from Lachema (Czech Republic). Ethanol used for $TiO_2$ sol preparation was dried using sodium, and then distilled. Phenol, provided by Reactivul (Romania), was used without further purification. The metal salts $LiNO_3$, $Zn(NO_3)_2 \cdot 6H_2O$, $Ce(NO_3)_3 \cdot 6H_2O$, $CrCl_3 \cdot 6H_2O$, $Co(NO_3)_3 \cdot 6H_2O$, $FeCl_3 \cdot 6H_2O$, $Al(NO_3)_3 \cdot 9H_2O$, $Cd(NO_3)_2 \cdot 4H_2O$ and $MnCl_2 \cdot 4H_2O$ (analytical grade, Lachema, Czech Republic) and $Na_2PtCl_6 \cdot 6H_2O$ (Fluka) were applied for

* Corresponding author. Tel.: +421 7 326 032; fax: +421 7 493 198; e-mail: brezova@cvtstu.cvt.stuba.sk


*PII* S1010-6030(97)00121-4

doped $TiO_2$ layer preparation. Deionized water was used in all the experiments.

### 2.2. Preparation of $TiO_2$ sol and $TiO_2$ supported on glass fibres

Commercial glass fibre fabric (for technical laminate application, Skloplast, Slovak Republic), with a specific weight of 500 g $m^{-2}$ and a fibre diameter of 13 μm, was used as support material. The coating surface layer (methacryl silane) of the technical glass fibre was removed by firing at 400 °C.

The $TiO_2$ sol corresponding to 5 wt.% of $TiO_2$ was synthesized by the sol–gel technique as described in Ref. [21]. The glass fibre fabric was dipped into the prepared $TiO_2$ sol. After removal, the layer was equilibrated for 2 days in the laboratory, and then stepwise calcined in a furnace, with 30 min steps every 100 °C including the top temperature of 450 °C, and freely cooled to room temperature. The concentration of titania in the supported photocatalyst was 10 mg per 1 g of glass fibre. The $TiO_2$ layers doped with metal ions were prepared analogously. The calculated amounts of metal salts were diluted directly in the prepared $TiO_2$ sol (the molar concentration of metal was evaluated in relation to titanium).

### 2.3. $M^{n+}/TiO_2$ photocatalyst characterization

The dependence of the ζ potential of the supported $M^{n+}/TiO_2$ photocatalysts on the pH was studied using an electrokinetic analyser (EKA-Paar, Austria) at a temperature of 25 °C. $NaNO_3$ was applied as the basic electrolyte (concentration, $10^{-4}$ M), and the pH values were maintained using 0.2 M HCl and 0.2 M NaOH [22].

The reflectance spectra of the supported $M^{n+}/TiO_2$ photocatalysts were measured using a UV–visible spectrophotometer (M40, Zeiss, Germany) equipped with a reflectance accessory with an integration sphere.

The X-ray powder patterns of $Pt/TiO_2$ were recorded using a DRON UM1 X-ray powder diffractometer with Bragg–Brentano parafocusing geometry equipped with a scintillation detector. Cu $K_\alpha$ radiation ($\lambda = 0.1542$ nm) was applied.

### 2.4. Photocatalytic experiments

The activity of the supported $M^{n+}/TiO_2$ photocatalysts (area, 1 $dm^2$) was tested using the reaction of phenol degradation. The reactions were performed in a photochemical immersion well (Applied Photophysics, UK) using a 125 W medium pressure mercury lamp (Applied Photophysics) as irradiation source. With the aim of inhibiting any direct photochemical process, wavelengths below 300 nm were removed using a Pyrex sleeve inserted in the central part of the photoreactor. The irradiated systems were continuously saturated by oxygen (flow rate, 100 ml $min^{-1}$). The experiments were carried out at a temperature of 50 °C. The pH values of the solutions were controlled by HCl and NaOH addition.

### 2.5. Product analysis

The concentrations of phenol and its degradation products, hydroquinone and catechol, in the irradiated samples were determined by high performance liquid chromatography (HPLC) (FPLC Pharmacia, Sweden) using a Separon SIX C-18 column (Tessek, Czech Republic) and a UV detector ($\lambda = 280$ nm). A mixture of methanol–water–$H_3PO_4$ (35 : 65 : 0.1) was applied as mobile phase.

UV spectra were measured using a UV–visible spectrophotometer (PU 8800, Philips) for all irradiated samples.

The concentration of phenol in the irradiated samples was also evaluated by the principal component regression (PCR) method [23,24]. The vector elements of the standard concentrations for phenol were determined by simultaneous measurement of the UV spectra and phenol concentration by HPLC in the analysed samples.

## 3. Results and discussion

### 3.1. Blank experiments

In the blank experiments, solutions with an initial phenol concentration of $c_0 = 1$ mM were irradiated without photocatalyst under identical conditions to those of the standard photocatalytic experiments (Pyrex sleeve, oxygen flow, temperature of 50 °C). During 60 min of irradiation, the concentration of phenol was monitored, and only negligible changes were observed. Thus the presence of $TiO_2$ photocatalyst is necessary for effective phenol decomposition on irradiation under the given experimental conditions.

### 3.2. Isoelectric point (IEP) determination

Figure 1 shows the dependence of the ζ potential on pH for $TiO_2$ and $Li^+/TiO_2$ (5 mol.% $Li^+ : Ti^{4+}$) photocatalysts supported on glass fibres using the sol–gel technique. For all the prepared $M^{n+}/TiO_2$ photocatalysts (5 mol.% $M^{n+} : Ti^{4+}$), the measured dependences of the ζ potential on pH are analogous to that depicted in Fig. 1. These were approximated by a quadratic function using the program SCIENTIST (MicroMath). The calculated values of the IEP are summarized in Table 1.

For the $M^{n+}/TiO_2$ photocatalysts prepared in our laboratory, the values of IEP are in the range 3.7–4.5, which is in agreement with IEP = 4–6 predicted for $TiO_2$ supported films [10]. As can be seen below, the changes in IEP do not directly reflect the photoactivity of $M^{n+}/TiO_2$ catalysts.

As the surface charge of $M^{n+}/TiO_2$ photocatalysts can substantially influence the adsorption of phenol ($pK_{phenol}$(25 °C) = 9.95 [25]), the effect of pH was studied in detail for $Pt^0/TiO_2$ photocatalysts at a temperature of 50 °C. The deg-

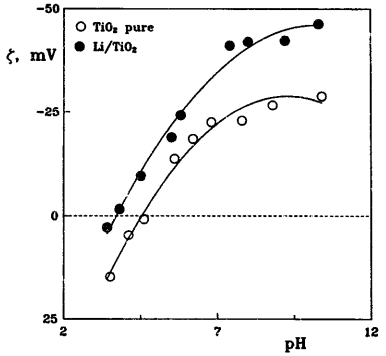


Fig. 1. Dependence of the $\zeta$ potential on the pH at 25 °C for $TiO_2$ photocatalysts supported by the sol–gel technique on glass fibres: ○, $TiO_2$; ●, $Li^+/TiO_2$ (5 mol.% $Li^+ : Ti^{4+}$).

Table 1
Isoelectric point (IEP) determined at 25 °C for $M^{n+}/TiO_2$ (5 mol.% $M^{n+} : Ti^{4+}$) photocatalysts supported by the sol–gel technique on glass fibres

| Photocatalyst | IEP |
|---|---|
| $TiO_2$ | 4.5 |
| $Li^+/TiO_2$ | 3.7 |
| $Zn^{2+}/TiO_2$ | 4.1 |
| $Cd^{2+}/TiO_2$ | 4.1 |
| $Pt^0/TiO_2$ | 4.4 |
| $Ce^{3+}/TiO_2$ | 3.8 |
| $Cr^{3+}/TiO_2$ | 3.8 |
| $Co^{3+}/TiO_2$ | 4.0 |
| $Fe^{3+}/TiO_2$ | 4.4 |
| $Al^{3+}/TiO_2$ | 4.1 |
| $Mn^{2+}/TiO_2$ | 4.0 |

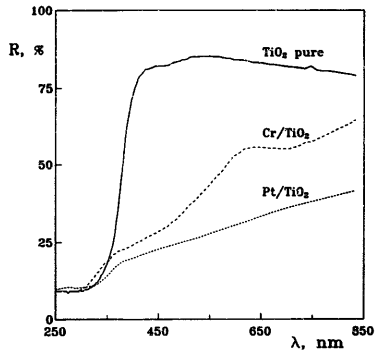


Fig. 2. Reflectance spectra of $TiO_2$ photocatalysts supported by the sol–gel technique on glass fibres: ———, $TiO_2$; – – –, $Cr^{3+}/TiO_2$; · · · ·, $Pt/TiO_2$ (5 mol.% $M^{n+} : Ti^{4+}$).

radation of phenol ($c_0 = 0.1$ mM) is very effective in acidic solution, and between pH 2.0 and pH 10.0 only small changes in the phenol degradation rate (evaluated as the formal phenol half-time $\tau_{1/2}$) are observed ($\tau_{1/2} \sim 10$ min). Similar results were reported by O'Shea and Cardona [26], suggesting only a minor influence of the variation of $H_3O^+$ and $OH^-$ concentrations on the overall degradation in this pH range. However, in solution at pH > 10, phenol degradation is significantly lower ($\tau_{1/2} > 20$ min), probably due to the hindered adsorption of phenoxide species on the negatively charged $Pt^0/TiO_2$ surface.

### 3.3. Reflectance spectra

The presence of metal dopant may also significantly influence the optical properties of the $TiO_2$ photocatalyst, and the light absorption of $M^{n+}/TiO_2$ can be shifted into the visible region [17]. The thermal treatment during $TiO_2$ preparation by the sol–gel technique determines whether anatase ($\lambda_{bg} = 380$ nm) or rutile ($\lambda_{bg} = 410$ nm) is formed [8,11].

The reflectance spectrum of $TiO_2$ supported on glass fibres by the sol–gel technique (Fig. 2) shows predominantly the anatase structure. In addition, the presence of anatase is confirmed by the X-ray powder pattern of $Pt/TiO_2$ (5 mol.% $Pt : Ti^{4+}$) shown in Fig. 7 (see later). Absorption in the visible region was measured for $M^{n+}/TiO_2$ photocatalysts (5 mol.% $M^{n+} : Ti^{4+}$) doped by $Fe^{3+}$, $Co^{3+}$, $Mn^{2+}$ and $Cr^{3+}$. A colour change for these layers was observed (Fig. 2). During the preparation of $Pt^0/TiO_2$, platinum was deposited on the $TiO_2$ surface, and the reflectivity of the photocatalyst was significantly decreased in the 400–850 nm region (Fig. 2).

### 3.4. Photocatalytic phenol degradation on $M^{n+}/TiO_2$

The rapid decrease in phenol concentration ($c_0 = 0.1$ mM) during irradiation at 50 °C using $TiO_2$ and $Pt^0/TiO_2$ (5 mol.% $Pt^0 : Ti^{4+}$) photocatalysts is depicted in Figs. 3(a) and 3(b). During irradiation, the simultaneous formation and decomposition of two intermediates, i.e. hydroquinone and catechol, may be monitored by HPLC (Figs. 3(a) and 3(b)). The relatively high concentration of hydroquinone observed after 30 min of irradiation using the $Pt^0/TiO_2$ catalyst is interesting.

The dependence of the phenol concentration $c$ on the irradiation time $t_{irr}$ was fitted (by the non-linear least-squares minimization procedure) to an exponential function

$$c = A + B\exp(-kt_{irr}) \quad (1)$$

using the program SCIENTIST (MicroMath). Formal first-order kinetics were proposed for phenol decomposition and the formal rate constant $k$ was evaluated. From this, the formal phenol half-times were calculated. The formal phenol half-times were used for a comparison of the efficiency of the photocatalytic process on $M^{n+}/TiO_2$.

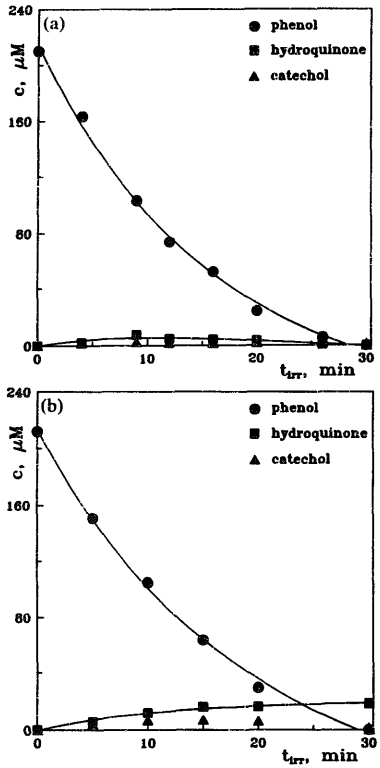


Fig. 3. Concentration changes during the irradiation of a phenol solution ($c_0 = 0.1$ mM) at a temperature of 50 °C: (a) $TiO_2$ photocatalyst; (b) $Pt^0/TiO_2$ photocatalyst (5 mol.% $Pt^0 : Ti^{4+}$).

The linear dependence of the formal phenol half-time $\tau_{1/2}$ on the initial concentration of phenol $c_0$ for $TiO_2$ photocatalysts is illustrated in Fig. 4. Such a kinetic behaviour is characteristic of the Langmuir–Hinshelwood description of the surface photocatalytic reactions in systems with constant oxygen concentration [7]

$$\tau_{1/2} = \frac{\ln 2}{k_1 k_2} + \frac{K_{ph}}{2k_1 k_2} c_0 \qquad (2)$$

where $K_{ph}$ is the adsorption constant of phenol and $k_1$ and $k_2$ are the formal experimental constants including the influence of the experimental arrangement and oxygen concentration [7].

Analogous linear dependences to those shown in Fig. 4 were also evaluated for $Li^+/TiO_2$, $Zn^{2+}/TiO_2$ and $Cd^{2+}/TiO_2$ photocatalysts (5 mol.% $M^{n+} : Ti^{4+}$). The calculated parameters of the lines obtained (intercept, slope, $R^2$) are summarized in Table 2, together with the values of the phenol adsorption constant $K_{ph}$. Comparing these values with the adsorption constant $K_{ph} = 4.07$ mM$^{-1}$ reported for phenol decomposition in aqueous $TiO_2$ suspension [27] and $K_{ph} = 8.9$ mM$^{-1}$ for $TiO_2$ P25 particles fixed on glass fibres [28], it can be seen that very good agreement is obtained for the $TiO_2$ supported photocatalysts. The relatively high value of the adsorption constant obtained for the photocatalyst doped with lithium ions ($K_{ph} = 27.7$ mM$^{-1}$) is remarkable.

On the other hand, $Co^{3+}/TiO_2$, $Cr^{3+}/TiO_2$, $Mn^{2+}/TiO_2$ and $Ce^{3+}/TiO_2$ photocatalysts (5 mol.% $M^{n+} : Ti^{4+}$) are photochemically inactive, and a very low activity of phenol degradation is observed for $Al^{3+}/TiO_2$ and $Fe^{3+}/TiO_2$, where the formal phenol half-times obtained for the lowest initial phenol concentration ($c_0 = 0.1$ mM) are 33 min and 44 min respectively.

The effect of individual metal ions on the photocatalytic activity of $M^{n+}/TiO_2$ is a complex problem. However, a significant decrease in the photocatalytic activity is observed for $M^{n+}/TiO_2$ doped with metal ions characterized by ionic radii comparable with the ionic radius of $Ti^{4+}$ [29], and by a more positive redox potential of the $M^{n+}/M^{(n-1)+}$ couple [30] than the band edge potential of the $TiO_2$ conduction band ($-0.4$ V vs. NHE at pH 7 [31]).

The characteristics of $Cr/TiO_2$ samples with various Cr concentrations were studied by electron paramagnetic resonance (EPR) spectroscopy, and the formation of large agglomerates of $Cr_2O_3$ was confirmed for $Cr/TiO_2$ materials doped in the range 3–5 wt.% [32]. Herrmann et al. [14] prepared homodispersed and homogeneously doped nanoporous $Ga^{3+}/TiO_2$, $Cr^{3+}/TiO_2$, $Sb^{5+}/TiO_2$ and $V^{5+}/TiO_2$ photocatalysts by the flame reactor method. All samples exhibited smaller photocatalytic activities than pure $TiO_2$ of a similar texture, and the strongest inhibitory effect was

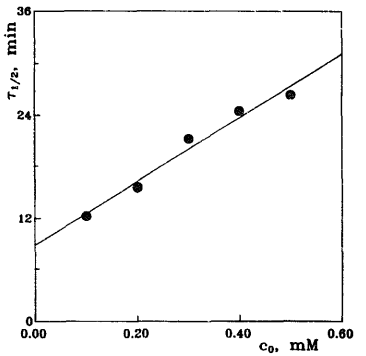


Fig. 4. Dependence of the formal phenol half-time on the initial phenol concentration for the photocatalytic degradation (temperature, 50 °C) on $TiO_2$ supported by the sol–gel technique on glass fibres.

Table 2
Calculated parameters for the linear dependence of the formal phenol half-time on the initial concentration of phenol, and values of the phenol adsorption constant (dopant concentration, 5 mol.% $M^{n+}$ : $Ti^{4+}$; photocatalytic experiments were carried out at 50 °C)

| Photocatalyst | $\tau_{1/2} = (\ln 2)/(k_1k_2) + [K_{ph}/(2k_1k_2)]c_0$ | | | |
|---|---|---|---|---|
| | $(\ln 2)/(k_1k_2)$ (min) | $K_{ph}/(2k_1k_2)$ (min $mM^{-1}$) | $R^2$ | $K_{ph}$ ($mM^{-1}$) |
| $TiO_2$ | 8.8 | 37.2 | 0.998 | 5.9 |
| $Li^+/TiO_2$ | 2.7 | 53.9 | 0.998 | 27.7 |
| $Zn^{2+}/TiO_2$ | 6.8 | 44.5 | 0.997 | 9.1 |
| $Cd^{2+}/TiO_2$ | 18.3 | 34.6 | 0.999 | 2.6 |

observed for $Cr^{3+}/TiO_2$. The detrimental effect of doping was explained by the fact that trivalent and pentavalent ions behave as recombination centres of the photoproduced charge carriers [14]. The $Fe^{3+}$ ion concentration is dominant for $Fe^{3+}/TiO_2$ materials [15,17,18]. $Fe^{3+}/TiO_2$ samples containing various amounts of $Fe^{3+}$ (0.2–10 wt.%) were applied to the photocatalytic oxidation of nitrite; the most photoactive sample was found to contain 0.5 wt.% $Fe^{3+}$ [18]. Similar results were obtained by Soria et al. [15] and Palmisano et al. [17] for $TiO_2$ samples doped with $Fe^{3+}$. For the more highly doped materials (iron concentration higher than 0.1% [17] or 0.5% [18]), the photoreactivity is negatively influenced by the presence of iron ions, probably due to a decrease in the density of surface-active centres.

We propose that the low photoactivity of the prepared $Co^{3+}/TiO_2$, $Cr^{3+}/TiO_2$, $Mn^{2+}/TiO_2$, $Ce^{3+}/TiO_2$, $Al^{3+}/TiO_2$ and $Fe^{3+}/TiO_2$ photocatalysts (5 mol.% $M^{n+}$ : $Ti^{4+}$) can be explained as discussed in Refs. [14–18].

### 3.5. Photocatalytic activity of $Pt^0/TiO_2$ with various dopant concentrations

Doped $Pt^0/TiO_2$ photocatalysts with platinum concentrations of 0.5, 1.25, 2.5, 3.75 and 5 mol.% $Pt^0$ : $Ti^{4+}$ were synthesized by the sol–gel technique on glass fibres. The effective decrease in phenol concentration during irradiation in the presence of the $Pt^0/TiO_2$ photocatalyst (3.75 mol.% $Pt^0$ : $Ti^{4+}$), in systems with increasing initial phenol concentration, is shown in Fig. 5. However, as noted above (Fig. 3(b)), the decomposition of the intermediates is slower than for dopant-free $TiO_2$ layers (Fig. 3(a)). The set of UV spectra obtained during irradiation in the presence of the $Pt^0/TiO_2$ photocatalyst (3.75 mol.% $Pt^0$ : $Ti^{4+}$; $c_0 = 0.3$ mM) clearly illustrates the formation of intermediates during 30 min of irradiation (Fig. 6). Consequently, longer irradiation times are necessary for the total mineralization of phenol using $Pt^0/TiO_2$ photocatalysts. In an effort to obtain information on the oxidation states of platinum in the prepared $Pt/TiO_2$ photocatalysts, the X-ray powder diffraction patterns were measured for a sample with a platinum concentration of 5 mol.% Pt : $Ti^{4+}$. The measured results were analysed by comparing the X-ray powder diffraction patterns with data published in the Powder Diffraction Files (PDFs) with the following numbers: Pt 4-802; $Pt_3O_4$ 21-1284; PtO 27-1331; $PtO_2$ 23-1306; PtTi 23-1310; $PtCl_4$ 19-914; $TiO_2$ (anatase) 21-1292; $TiO_2$ (rutile) 21-1276. Our data (Fig. 7) confirm the formation of the anatase structure during the preparation

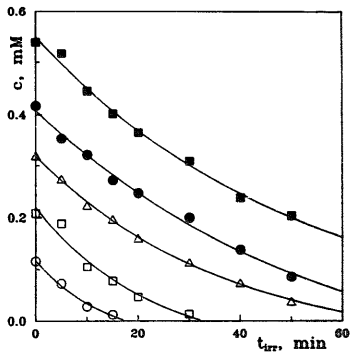


Fig. 5. Decrease in phenol concentration during irradiation at 50 °C in the presence of a $Pt^0/TiO_2$ photocatalyst (3.75 mol.% $Pt^0$ : $Ti^{4+}$) in systems with various initial phenol concentrations $c_0$: ■, 0.5 mM; ●, 0.4 mM; △, 0.3 mM; □, 0.2 mM; ○, 0.1 mM.

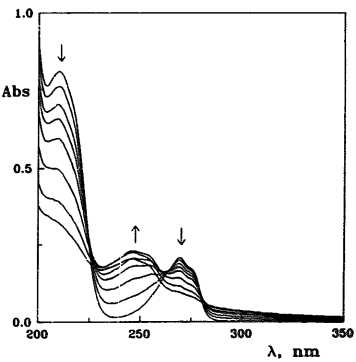


Fig. 6. Changes in the UV spectra observed during photocatalytic phenol decomposition on $Pt^0/TiO_2$ (3.75 mol.% $Pt^0$ : $Ti^{4+}$) ($c_0 = 0.3$ mM; temperature, 50 °C). Irradiation time: 0, 5, 10, 15, 20, 25, 30 and 45 min.

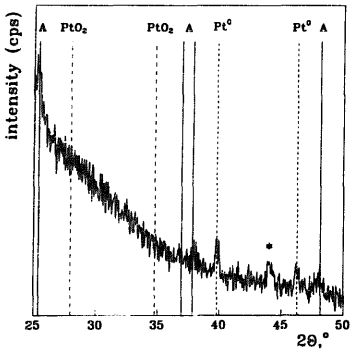


Fig. 7. X-Ray powder diffraction pattern of $Pt/TiO_2$ photocatalyst supported by the sol–gel technique on glass fibres (5 mol.% $Pt : Ti^{4+}$) with marked lines for anatase A (———), $PtO_2$ (– – –) and $Pt^0$ (- - -). Conditions: step, 0.04° 2θ; time of step, 15 s. Asterisk represents the signal of the carrier material.

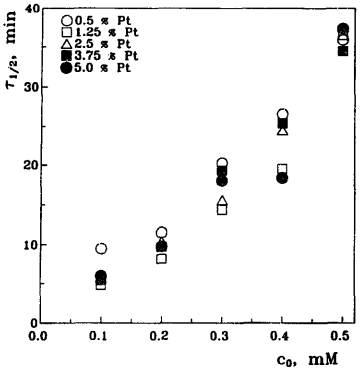


Fig. 8. Dependence of the formal phenol half-time on the initial phenol concentration for the photocatalytic degradation (temperature, 50 °C) on $Pt^0/TiO_2$ photocatalysts at various $Pt^0$ concentrations (mol.% $Pt^0 : Ti^{4+}$).

of a $TiO_2$ layer on glass fibre, and show unambiguously the presence of $Pt^0$ in the sample. Signals representing platinum in the higher oxidation states were not found.

The positive role of platinum [14,16,19,33] and of Pd, Ir, Rh, Os and Ru [16,19,34] loading on $TiO_2$ in the photocatalytic decomposition of organic compounds has been described previously. Kaise et al. [19] reported, for $Pt^0/TiO_2$, an optimal loading of metal in the range 0.5–1.5 mmol $M^{n+} : TiO_2$ for effective radical formation. Herrmann et al. [14] obtained a hyperbolic decrease in the reaction rate with increasing $Pt^0$ loading on $TiO_2$, and the experimental results were interpreted by the transfer of photoelectrons from the semiconductor to the metal particles, and by the decrease in the amount of oxygen photoadsorbed on $TiO_2$ as a negatively charged species with increasing $Pt^0$ content. The role of the number and size of Pt clusters on $TiO_2$ has also been discussed by Gerischer and coworkers [35,36] and Sadeghi et al. [37].

The dependence of the formal phenol half-time on the initial phenol concentration is non-linear for $Pt^0/TiO_2$ photocatalysts, as depicted in Fig. 8. Consequently, the kinetic equation (Eq. (2)) is not valid for $Pt^0/TiO_2$, and platinum is probably included in the oxygen reactions on the $TiO_2$ surface as proposed in Refs. [14,35–38].

In addition, in our experiments, the concentration of $Pt^0$ substantially influences the photoactivity of $Pt^0/TiO_2$; the best properties were obtained for a platinum content of 1.25 mol.% $Pt^0 : Ti^{4+}$. Concentrations of $Pt^0$ of more than 5 mol.% $Pt^0 : Ti^{4+}$ have a detrimental effect on the photocatalyst activity.

## 4. Conclusions

The presence of metals, such as $Li^+$, $Zn^{2+}$, $Cd^{2+}$, $Pt^0$, $Co^{3+}$, $Ce^{3+}$, $Cr^{3+}$, $Mn^{2+}$, $Al^{3+}$ and $Fe^{3+}$, may significantly change the photoactivity of a $TiO_2$ layer prepared on glass fibre by the sol–gel technique. The prepared dopant-free $TiO_2$ photocatalyst is very effective in the reaction of phenol decomposition, and a linear dependence of the formal phenol half-time on the initial concentration of phenol in solution is found. An analogous linear dependence (from which the corresponding phenol adsorption constants were calculated and compared) is also obtained for $Li^+/TiO_2$, $Zn^{2+}/TiO_2$ and $Cd^{2+}/TiO_2$ photocatalysts.

The photoactivity is dependent on the dopant concentration for $Pt^0/TiO_2$ materials with a platinum content in the range 0.5–5.0 mol.% $Pt^0 : Ti^{4+}$. In our experiments, the best results were obtained for a $Pt^0/TiO_2$ photocatalyst with 1.25 mol.% $Pt^0 : Ti^{4+}$. However, the degradation of hydroquinone, produced as an intermediate, is slower than for dopant-free $TiO_2$ photocatalyst. Consequently, longer irradiation times are necessary for the total mineralization of phenol using $Pt^0/TiO_2$ photocatalysts.

The presence of $Co^{3+}$, $Ce^{3+}$, $Cr^{3+}$, $Mn^{2+}$, $Al^{3+}$ and $Fe^{3+}$ ions (5 mol.% $M^{n+} : Ti^{4+}$) in the $TiO_2$ layer supported on glass fibres by the sol–gel technique has a detrimental effect on the photoactivity.

## Acknowledgements

We thank the Slovak Grant Agency for financial support (Projects 1/1397/4 and 1/1425/94).

## References

[1] D.F. Ollis, H. Al-Ekabi (Eds.), Photocatalytic Purification and Treatment of Water and Air, Elsevier, Amsterdam, 1993.
[2] O. Legrini, E. Oliveros, A.M. Braun, Chem. Rev. 93 (1993) 671.

[3] M.R. Hoffmann, S.T. Martin, W. Choi, D.W. Bahnemann, Chem. Rev. 95 (1995) 69.
[4] G.R. Helz, R.G. Zepp, D.G. Crosby (Eds.), Aquatic and Surface Photochemistry, Lewis Publishers, CRC, Boca Raton, 1994.
[5] R.W. Matthews, Solar Energy 38 (1987) 405.
[6] R.W. Matthews, J. Phys. Chem. 91 (1987) 3328.
[7] J. Sabate, M.A. Anderson, H. Kikkawa, M. Edwards, C.G. Hill Jr., J. Catal. 127 (1991) 157.
[8] S. Tunesi, M.A. Anderson, J. Phys. Chem. 95 (1991) 3399.
[9] M.A. Aguado, M.A. Anderson, Solar Energy Mater. Solar Cells 28 (1993) 45.
[10] D.H. Kim, M.A. Anderson, J. Photochem. Photobiol. A: Chem. 94 (1996) 221.
[11] B. Ohtani, S. Zhang, J. Handa, H. Kajiwara, S. Nishimoto, T. Kagiya, J. Photochem. Photobiol. A: Chem. 64 (1992) 223.
[12] M.A. Fox, K.E. Doan, M.T. Dulay, Res. Chem. Intermed. 20 (1994) 711.
[13] X.-Z. Ding, Y.-Z. He, J. Mater. Sci. Lett. 15 (1996) 320.
[14] J.-M. Herrmann, W. Mu, P. Pichat, in: M. Guisnet, J. Barrault, C. Bouchoule, D. Duprez, G. Perot, R. Maurel, (Eds.), Heterogeneous Catalysis and Fine Chemicals II, Elsevier, Amsterdam, 1991.
[15] J. Soria, J.C. Conesa, V. Augugliaro, L. Palmisano, M. Schiavello, A. Sclafani, J. Phys. Chem. 95 (1991) 274.
[16] B. Ohtani, M. Kakimoto, S. Nishimoto, T. Kagiya, J. Photochem. Photobiol. A: Chem. 70 (1993) 265.
[17] L. Palmisano, M. Schiavello, A. Sclafani, C. Martin, I. Martin, V. Rives, Catal. Lett. 24 (1994) 303.
[18] A. Milis, J. Peral, X. Domenech, J.A. Navío, J. Mol. Catal. 87 (1994) 67.
[19] M. Kaise, H. Nagai, K. Tokuhashi, S. Kondo, S. Nimura, O. Kikuchi, Langmuir 10 (1994) 1345.
[20] K.E. Karakitsou, X.E. Verykios, J. Phys. Chem. 97 (1993) 1184.
[21] M. Mikula, V. Brezová, M. Čeppan, L. Pach, Ľ. Karpinský, J. Mater. Sci. Lett. 14 (1995) 615.
[22] V. Brezová, A. Staško, S. Biskupič, A. Blažková, B. Havlínová, J. Phys. Chem. 98 (1994) 8977.
[23] H. Martens, T. Naes, Multivariate Calibration, Wiley, Chichester, 1989, p. 97.
[24] V. Brezová, E. Brandšteterová, M. Čeppan, J. Pieš, Collect. Czech. Chem. Commun. 58 (1993) 1285.
[25] T.I. Temnikovova, Theoretical Fundamentals of Organic Chemistry, Publishing House of the Slovak Academy of Sciences, Bratislava, 1992, p. 207.
[26] K.E. O'Shea, C. Cardona, J. Photochem. Photobiol. A: Chem. 91 (1995) 67.
[27] V. Augugliaro, L. Palmisano, A. Sclafani, C. Minero, E. Pelizzetti, Toxicol. Environ. Chem. 16 (1988) 89.
[28] V. Brezová, A. Blažková, M. Breznan, P. Kottáš, M. Čeppan, Collect. Czech. Chem. Commun. 60 (1995) 788.
[29] F.A. Cotton, G. Wilkinson, Inorganic Chemistry, Academia, Praha, 1973, p. 56.
[30] V. Kellö, A. Tkáč, Physical Chemistry, Alfa, Bratislava, 1969, pp. 497–499.
[31] H. Yoneyama, Crit. Rev. Solid State Mater. Sci. 18 (1993) 69.
[32] K. Köhler, C.W. Schläpfer, A. von Zelewsky, J. Nickl, J. Engweiler, A. Baiker, J. Catal. 143 (1993) 201.
[33] I. Izumi, W.W. Dunn, K.O. Wilbourn, F.-R. Fan, A.J. Bard, J. Phys. Chem. 84 (1980) 3207.
[34] J. Papp, H.-S. Shen, R. Kershaw, K. Dwight, A. Wold, Chem. Mater. 5 (1993) 284.
[35] C.-M. Wang, A. Heller, H. Gerischer, J. Am. Chem. Soc. 114 (1992) 5230.
[36] H. Gerischer, A. Heller, J. Phys. Chem. 95 (1991) 5261.
[37] M. Sadeghi, W. Liu, T.-G. Zhang, P. Stavropoulos, B. Levy, J. Phys. Chem. 100 (1996) 19 466.
[38] P. Pichat, J.-M. Herrmann, in: N. Serpone, E. Pelizzetti (Eds.), Photocatalysis. Fundamentals and Applications, Wiley, New York, 1989, pp. 218–250.